Nanoscale

Cu Nanowire-Catalyzed Electrochemical Reduction of CO or CO2

Journal:	*Nanoscale*
Manuscript ID	NR-COM-04-2019-003170.R1
Article Type:	Communication
Date Submitted by the Author:	25-May-2019

Complete List of Authors:	Zhang, Hongyi; Brown University, Chemistry Zhang, Yinjia; Brown University, School of Engineering Li, Yuyang; Brown University, Chemistry Ahn, Stephen; Brown University, School of Engineering Palmore, G Tayhas; Brown University, School of Engineering Fu, Jiaju; Brown University, Chemistry Peterson, Andrew; Brown University, School of Engineering Sun, Shouheng; Brown University, Chemistry

Journal Name

COMMUNICATION

Cu Nanowire-Catalyzed Electrochemical Reduction of CO or CO_2

Received 00th January 20xx,
Accepted 00th January 20xx

DOI: 10.1039/x0xx00000x

www.rsc.org/

Hongyi Zhang,[a] Yinjia Zhang,[b] Yuyang Li,[a] Stephen Ahn,[b] G. Tayhas R. Palmore,[b] Jiaju Fu,[a] Andrew A. Peterson,[b] Shouheng Sun[a,*]

We prepared micrometer long Cu nanowires (NWs) of 25 and 50 nm diameters and studied their electrocatalysis for electrochemical reduction of CO/CO_2 in 0.1 M $KHCO_3$ at room temperature. The 50 nm NWs show better selectivity than the 25 nm NWs, and catalyze CO reduction to C_2-hydrocarbons (C_2H_4 + C_2H_6) with a combined Faradaic efficiency (FE) of 60% (C_2H_4 FE of 35% and mass activity of 4.25A/gCu) at −1.1 V (vs reversible hydrogen electrode). The NW-catalyzed CO_2 reduction is less efficient due to the extra CO_2 to CO step required for the formation of C_2-hydrocarbons. These experimental evidence combined with DFT calculations suggest that CO is an important intermediate and NWs provide large Cu (100) surface for *CO hydrogenation (to *CHO) and *CO-*CHO coupling, leading to more selective reduction of CO than CO_2 towards C_2-hydrocarbons.

The accelerated consumption of fossil fuels required to maintain the fast pace of industrialization has led to increasing levels of CO_2 in the atmosphere, which raises the alarm about the stability of our environment and the energy sustainability. One obvious solution to this dilemma is to capture the CO_2 and convert it to reusable forms of carbon. Among the numerous methods developed for CO_2 conversion, electrochemical reduction of CO_2 is attractive for its ambient reaction conditions and its potential to be highly selective for a targeted product.[1,2] Electrochemical reduction of CO_2 in buffered solutions of $KHCO_3$ has been shown to be selective at forming CO[3-6] or formate,[8-13] but not so selective toward C_2 products because of the difficulty at controlling multi-electron reductions, hydrogenations, and carbon-carbon (C-C) coupling reactions, all of which are required for the conversion.

Copper (Cu) is a metal that can catalyze the electrochemical reduction of CO_2 to hydrocarbons. Earlier studies on single crystal Cu electrodes show that the Cu (100) surface tends to catalyze a C-C coupling reaction to yield ethylene (C_2H_4) with a reaction Faradaic efficiency (FE) of 40.7%, while the Cu (111) surface promotes the formation of methane (CH_4) with a FE of 50.5%.[14] In these reaction pathways, the adsorbed CO is believed to be an essential intermediate.[15-19] Under typical experimental conditions, however, C_2H_4 and CH_4 are always concurrently produced at Cu.[20] A Cu nanowire (NW) possesses a five-twinned surface structure exposing five (100) planes,[21,22] and should serve as a more selective catalyst for CO_2 reduction to C_2H_4. We prepared 25 and 50 nm wide Cu NWs and tested them for electrochemical reduction of CO or CO_2. The 50 nm NWs were more active and selective than the 25 nm ones at converting CO to C_2-hydrocarbons, and at -1.1 V (*vs* reversible hydrogen electrode (RHE)), the reduction yielded C_2H_4 + C_2H_6 with a combined FE of 60% (C_2H_4 FE of 35% and mass activity at 4.25A/gCu). The NWs were less efficient for the reduction of CO_2, but the C_2H_4 was still the main gas product (22% FE at -1.5 V). Density functional theory (DFT) calculations suggest that presence of CO on the Cu(100) surface facilitates *CO-*CHO coupling for the formation of C_2-hydrocarbons.

The Cu NWs were prepared by reducing CuCl in a heated oleylamine solution[23] (see supporting information, **SI**). To ensure the growth of good quality NWs, the reaction mixture was left unstirred once the solution turned red, which is similar to what was reported in the syntheses of Au[24] and FePt NWs,[25] where the oleylamine medium is believed to form reverse micelle-like cylinder-channels to facilitate the growth of NWs. In the current procedure, oleylamine served both as a reducing agent (to reduce CuCl to Cu) and as a stabilizer of the growing NWs. Different reaction conditions were tested to optimize NW growth. Temperatures over 200°C usually led to aggregated nanoparticles, but temperatures below 180°C did not yield good quality Cu NWs. Prolonged heating (> 2 h) degraded the quality of the Cu NWs. Therefore, the optimal temperature for preparing good quality Cu NWs was 190°C in less than 2 h. The 25 nm wide Cu NWs were obtained by heating the reaction mixture at 190°C for 0.5 h and 50 nm wide Cu NWs were obtained by heating the reaction mixture at 200°C for 1.5 h. **Figure 1** shows transmission electron microscopy (TEM) images of the two types of Cu NWs

[a] *Department of Chemistry, Brown University, Providence, Rhode Island 02912, United States. E-mail: ssun@brown.edu*
[b] *School of Engineering, Brown University, Providence, Rhode Island 02912, United States.*
Electronic Supplementary Information (ESI) available. See DOI: 10.1039/x0xx00000x

prepared. The NWs are micrometers in length with average widths of either 25 nm (**Figure 1a**) or 50 nm (**Figure 1b**), and (200) interfringe distances measured to be 0.19 nm (**Figure 1c**) and 0.18 nm (**Figure 1d**). The X-ray diffraction (XRD) patterns of the representative 25 nm and 50 nm wide Cu NWs (**Figure S1**) show that the Cu NWs has a face-centered cubic structure with the (200) inter-planar distance measured to be 0.18 nm, supporting what were measured in **Figure 1c,d**). The diffraction pattern does not show obvious copper oxide peaks, which indicates that the synthesis leads to the formation of metallic Cu NWs.

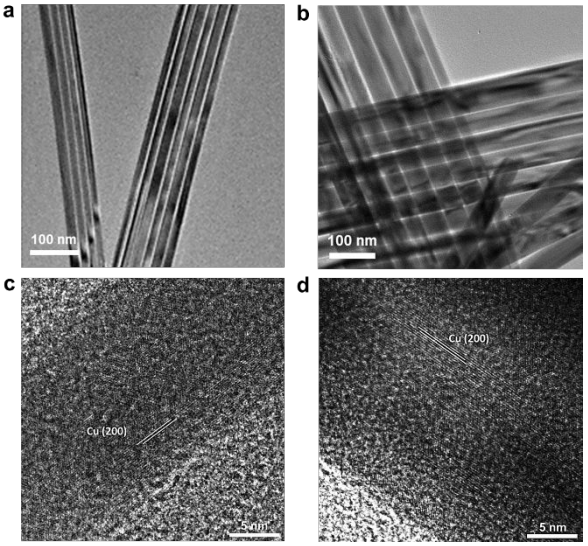

Figure 1. TEM images of (**a**) 25 nm and (**b**) 50 nm wide Cu NWs, and HRTEM images of a representative part of (**c**) 25 nm and (**d**) 50 nm Cu NW. (200) interplanar fringe distances were measured to be 0.19 nm (**c**) and 0.18 nm (**d**) respectively.

To test electrochemical and electrocatalytic properties of the Cu NWs, the NWs were deposited on a carbon support (Ketjen EC300J) at a mass ratio of 1:1 as described previously.[3] The carbon-supported NWs were subsequently immersed in n-butylamine under an atmosphere of N_2 at room temperature for two days to remove the oleylamine surfactant. The supported NWs were washed with ethanol and distilled water, and then dried at 80°C in a vacuum oven overnight. The resulting C-Cu catalysts (25 nm Cu NW and 50 nm Cu NW denoted as C-Cu-25 and C-Cu-50 (**Figure S2**), and were characterized by infrared (IR) spectroscopy: a representative spectrum of C-Cu-50 shows peaks characteristic of alkylamine (e.g., C–N stretching mode at 1375 cm^{-1}, CH_2 bending vibration at 1459 cm^{-1}, and CH_2 and CH_3 symmetric and asymmetric stretching vibrations within the range of 2840–3000 cm^{-1}) are absent (**Figure S3)**, indicating a successful replacement of oleylamine and removal of butylamine after washing and vacuum drying steps. Carbon ink was prepared by mixing C-Cu, polyvinylidene fluoride (PVDF) and a few drops of N-methyl-2-pyrrolidone (NMP) (**SI**). The ink was pasted onto carbon paper, dried under vacuum, and used as a working electrode.

Cyclic voltammetry (CV) shows that electrodes fabricated with C-Cu-50 and C-Cu-25 have two anodic peaks attributed to the oxidation of Cu(0) to Cu(I) and Cu(I) to Cu(II), and two cathodic peaks attributed to the reduction of Cu(II) to Cu(I), and Cu(I) to Cu(0) (**Figure 2a**).[26] The redox peaks at 0.65 V and 0.1 V, which are related to Cu(I)/Cu(0), are nearly independent on the NW diameter. In contrast, those associated with the Cu(II)/Cu(I) shift from 0.95 V (for the C-Cu-25) to 1.01 V (for the C-Cu-50), and from 0.4 V (for the C-Cu-25) to 0.45 V (for the C-Cu-50). The 50 nm Cu NWs appear to better stabilize the Cu(II) species than the 25 nm Cu NWs. **Figure 2b** shows the linear sweep voltammetry (LSV) curves of the C-Cu-50 measured under an atmosphere of Ar or CO. The C-Cu-50 exhibits a more obvious increase in cathodic current under Ar than CO. Similar behavior was observed on the C-Cu-25 (**Figure S4**). This result indicates that in the presence of CO, the Cu surface is covered by CO, which suppresses the hydrogen evolution reaction.

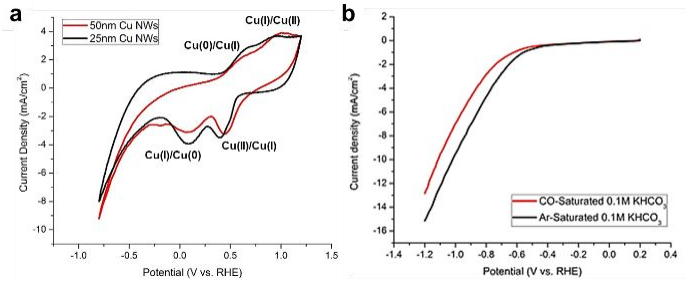

Figure 2. (**a**) CV of C-Cu-25 and C-Cu-50 in Ar-saturated 0.1 M $KHCO_3$. Scan rate = 50 mV/s. (**b**) LSV scans of C-Cu-50 in Ar- or CO-saturated 0.1 M $KHCO_3$. Scan rate = 5 mV/s.

The electrocatalytic reduction of CO was studied in a conventional H-cell (separated by a Nafion 212 membrane) filled with 0.1 M $KHCO_3$ solution (pH = 8.3) and saturated with CO at room temperature. Based on linear sweep voltammetry (**Figure 2b**), the applied reduction potentials were set from -0.7 V and beyond to obtain measurable amount of products. The gaseous products analyzed by gas chromatography (GC) contained C_2H_4, C_2H_6 and H_2 with a net FE of 100%±3% and the combined FE of C_2H_4 + C_2H_6 given in **Figure 3a**. No liquid products were detected by ^1H NMR at all potentials studied. At -1.1 V, the C-NW-50 catalyst produces more selectively C_2-hydrocarbons, C_2H_4 + C_2H_6, with a combined FE of 60%, in which the FE of C_2H_4 is at 35% (**Figure 3a**) and the related mass activity is at 4.25 A/gCu (**Figure 3b**). As a comparison, the C-NW-25 is less active than the C-Cu-50 (**Figure 3b**). Under the 8 h electrochemical reduction testing condition, the 50 nm NWs showed no obvious morphology changes (**Figure S5**). CH_4 was not detected under the current electrocatalysis condition, demonstrating high activity/selectivity of our C-Cu-50 towards C_2-hydrocarbons, which is different from what was reported.[27] When CO was replaced by CO_2, the reduction became less efficient and yielded CO, formate and C_2H_4 (**Figure 3c)**, as well as a trace amount of CH_4 (FE below 0.5%). C_2H_4 became a major product only when the reduction potentials reached beyond -1.3 V.

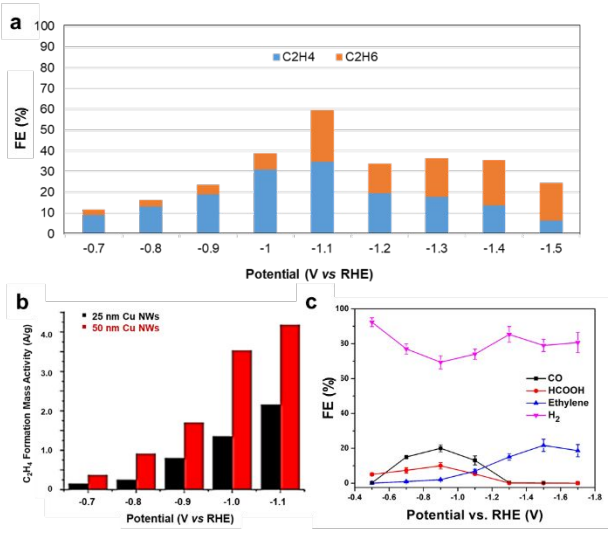

Figure 3. (**a**) FE of C_2H_4 + C_2H_6 from the C-Cu-50 catalyzed CO reduction at various reduction potentials. (**b**) Mass activities for the formation of C_2H_4 on the C-Cu-50 and C-Cu-25 catalysts. (**c**) FE of the CO_2 reduction products on C-Cu-50.

Previous reports on pH-dependent electrocatalytic reduction of CO on Cu surfaces showed that the catalytic selectivity towards C_2H_4 was improved when the solution pH was increased from 7 to 13.[27,28] In our reaction condition, the pH of the electrolyte after the reduction of CO varied only between 8.6 to 9.3 over the potential range studied. This 0.7 pH value change should not account for the selective formation of C_2H_4. Moreover, no CH_4 was detected in the NW-catalyzed reduction process. Therefore, we can conclude that 50 nm Cu NWs are especially selective for the CO reduction to C_2-hydrocarbons (C_2H_4 + C_2H_6).

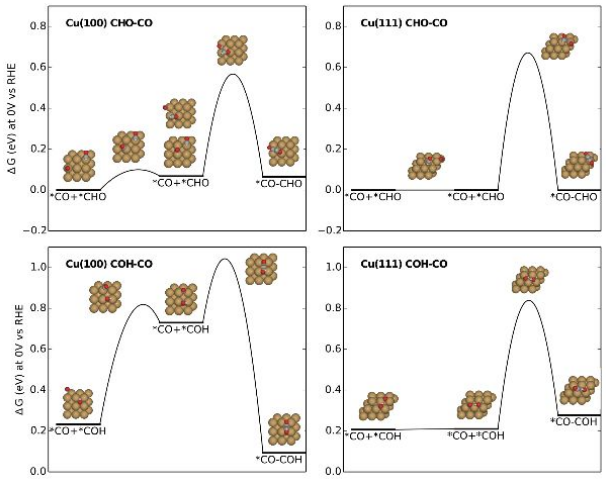

Figure 4. The free energy diagram of the CHO-CO and COH-CO coupling processes on Cu(100) and Cu(111) surfaces. Configurations are shown along the reaction pathway (Copper: Cu; red: O; grey: C; white: H). The higher initial energy of CO+COH reflects the calculated instability of COH relative to CHO.

The data collected from the electrochemical reduction of CO/CO_2 suggest that CO is an important intermediate for the formation of C_2-hydrocarbons on the Cu NW surface. The CO_2 reduction is less efficient than the CO reduction due likely to the required the first step conversion of CO_2 to CO. Density functional theory (DFT) was used to gain additional insight into possible C-C coupling pathways on Cu NWs, where five-twinned structure can expose five (100) planes around each NW.[21,22] The coupling reaction to produce CO-CO has been proposed as the rate determining step in C_2H_4 formation.[29,30] However, our calculations show that the CO-CO coupling barrier is high at 1.19 eV, even on the Cu(100) surface. Theoretical studies have further shown that a higher coverage of CO,[31] aqueous electrolyte environment,[32-35] and degree of hydrogenation of the CO-based adsorbate[16] can reduce the barrier to C-C coupling. Here, we used the climbing-image NEB method to compare the activation barrier energies of CHO-CO and COH-CO coupling on Cu(100) and Cu(111) surfaces. The results from these calculations are shown in **Figure 4**. In all cases, the first barrier reflects diffusion of the two adsorbates moving closer to each other, and the second barrier is the C-C bond-forming step. Among the four cases, the CHO-CO coupling on Cu(100) has the lowest total barrier, about 0.1 eV lower than that the same reaction on Cu(111) and on Cu(211).[16] Interestingly, for COH-CO coupling on Cu(100), the major contribution to the barrier is the initial diffusion process, although the total barrier is much higher than the CO-CHO coupling. If high levels of CO and COH coverage are encountered during CO_2 reduction, the diffusion barrier may drop greatly. Consequently, there may be a switch from CHO-CO pathway to COH-CO pathway on Cu(100) as coverage increases. In either case, the Cu(100) facet has a lower activation barrier than Cu(111).

In summary, micrometer long Cu NWs with 25 nm and 50 NWs diameters were prepared for electrochemical reduction of CO/CO_2 to C_2-hydrocarbons. With the exception of hydrogen evolution reaction on Cu, the 50 nm NWs show higher activity and selectivity than the 25 nm NWs toward C_2-hydrocarbon gas products C_2H_4 + C_2H_6 with a combined FE of 60% at -1.1 V. neither CH_4 nor other liquid products are detected in the CO reduction process. The NWs are less efficient for the CO_2 reduction, yielding CO + formate and C_2H_4 with a combined FE <35% at -0.9 V, and C_2H_4 being a dominant gas product (22% FE) only at -1.5 V. Our studies demonstrate great potentials of Cu NWs as a selective catalyst for CO/CO_2 reduction to C_2-hydrocarbons, and CO is an important intermediate for C-C coupling in the hydrocarbon formation process. We are working to solve the stability issue and to develop Cu NWs as an efficient catalyst for electrochemical reduction of CO_2 to hydrocarbons.

Acknowledgement: The work was supported by the American Chemical Society Petroleum Research Fund (57114-ND5) and in part by the Center for the Capture and Conversion of CO_2, a

Center for Chemical Innovation funded by the National Science Foundation, CHE-1240020.

References

1. Hori, Y. Modern aspects of electrochemistry. Springer New York, **2008**, 89-189.
2. Whipple, D. T.; Kenis, P. J., Prospects of CO_2 utilization via direct heterogeneous electrochemical reduction. *J. Phys. Chem Lett.* **2010**, 1, 3451-3458.
3. Zhu, W.; Zhang, Y.-J.; Zhang, H.; Lv, H.; Li, Q.; Michalsky, R.; Peterson, A. A.; Sun, S., Active and selective conversion of CO_2 to CO on ultrathin Au nanowires. *J. Am. Chem. Soc*. **2014**, 136, 16132-16135.
4. Kim, C.; Jeon, H. S.; Eom, T.; Jee, M. S.; Kim, H.; Friend, C. M.; Min, B. K.; Hwang, Y. J., Achieving selective and efficient electrocatalytic activity for CO_2 reduction using immobilized silver nanoparticles. *J. Am. Chem. Soc*. **2015**, 137, 13844-13850.
5. Rosen, J.; Hutchings, G. S.; Lu, Q.; Forest, R. V.; Moore, A.; Jiao, F., Electrodeposited Zn dendrites with enhanced CO selectivity for electrocatalytic CO_2 reduction. *ACS Catal.* **2015**, 5, 4586-4591.
6. Li, Q.; Fu, J. J.; Zhu, W. L.; Chen, Z. Z.; Shen, B.; Wu, L. H.; Xi, Z.; Wang, T. Y.; Lu, G.; Zhu, J. J.; Sun, S. H., Tuning Sn-Catalysis for Electrochemical Reduction of CO_2 to CO via the Core/Shell Cu/SnO_2 Structure. *J. Am. Chem. Soc*. **2017**, 139, 4290-4293.
7. Hou, P.; Wang, X.; Wang, Z.; Kang, P., Gas Phase Electrolysis of Carbon Dioxide to Carbon Monoxide Using Nickel Nitride as the Carbon Enrichment Catalyst. *ACS Appl. Mater. Interf*. **2018**, *10*, 38024–38031.
8. Chen, Y.; Kanan, M. W., Tin oxide dependence of the CO_2 reduction efficiency on tin electrodes and enhanced activity for tin/tin oxide thin-film catalysts. *J. Am. Chem. Soc.* **2012**, *134*, 1986-1989.
9. Zhang, S.; Kang, P.; Meyer, T. J., Nanostructured tin catalysts for selective electrochemical reduction of carbon dioxide to formate. *J. Am. Chem. Soc.* **2014**, 136, 1734-1737.
10. Kortlever, R.; Peters, I.; Koper, S.; Koper, M. T., Electrochemical CO_2 reduction to formic acid at low overpotential and with high faradaic efficiency on carbon-supported bimetallic Pd–Pt nanoparticles. *ACS Catal*. **2015**, 5, 3916-3923.
11. Kumar, B.; Atla, V.; Brian, J. P.; Kumari, S.; Nguyen, T. Q.; Sunkara, M.; Spurgeon, J. M., Reduced SnO_2 Porous Nanowires with a High Density of Grain Boundaries as Catalysts for Efficient Electrochemical CO_2 -into-HCOOH Conversion. *Angew. Chem. Int. Ed. Eng.* **2017**, *56*, 3645-3649.
12. Daiyan, R.; Lu, X.; Saputera, W. H.; Ng, Y. H.; Amal, R., Highly Selective Reduction of CO_2 to Formate at Low Overpotentials Achieved by a Mesoporous Tin Oxide Electrocatalyst. *ACS Sust. Chem. Eng.* **2018**, *6*, 1670-1679.
13. Jiang, B.; Zhang, X. G.; Jiang, K.; Wu, D. Y.; Cai, W. B., Boosting Formate Production in Electrocatalytic CO_2 Reduction over Wide Potential Window on Pd Surfaces. *J. Am. Chem. Soc.* **2018**, *140*, 2880-2889.
14. Hori, Y.; Takahashi, I.; Koga, O.; Hoshi, N., Selective formation of C2 compounds from electrochemical reduction of CO_2 at a series of copper single crystal electrodes. *J. Phys. Chem. B* **2002**, *106*, 15-17.
15. Peterson, A. A.; Abild-Pedersen, F.; Studt, F.; Rossmeisl, J.; Nørskov, J. K., How copper catalyzes the electroreduction of carbon dioxide into hydrocarbon fuels. *Energy Environ. Sci.* **2010**, *3*, 1311-1315.
16. Montoya, J. H.; Peterson, A. A.; Nørskov, J. K., Insights into C-C Coupling in CO_2 Electroreduction on Copper Electrodes. *ChemCatChem* **2013**, *5*, 737-742.
17. Li, C. W.; Ciston, J.; Kanan, M. W., Electroreduction of carbon monoxide to liquid fuel on oxide-derived nanocrystalline copper. *Nature* **2014**, *508*, 504-507.
18. Huang, Y.; Handoko, A. D.; Hirunsit, P.; Yeo, B. S., Electrochemical Reduction of CO_2 Using Copper Single-Crystal Surfaces: Effects of CO* Coverage on the Selective Formation of Ethylene. *ACS Catal.* **2017**, *7*, 1749-1756.
19. Wang, L.; Nitopi, S. A.; Bertheussen, E.; Orazov, M.; Morales-Guio, C. G.; Liu, X. Y.; Higgins, D. C.; Chan, K. R.; Norskov, J. K.; Hahn, C.; Jaramillo, T. F., Electrochemical Carbon Monoxide Reduction on Polycrystalline Copper: Effects of Potential, Pressure, and pH on Selectivity toward Multicarbon and Oxygenated Products. *ACS Catal*. **2018**, *8*, 7445-7454.
20. Roberts, F. S.; Kuhl, K. P.; Nilsson, A., High selectivity for ethylene from carbon dioxide reduction over copper nanocube electrocatalysts. *Angew. Chem. Int. Ed*. **2015**, *54*, 5179-5182.
21. Xia, Y.; Xiong, Y.; Lim, B.; Skrabalak, S. E., Shape-controlled synthesis of metal nanocrystals: simple chemistry meets complex physics? *Angew. Chem. Int. Ed*. **2009**, *48*, 60-103.
22. Yang, H.-J.; He, S.-Y.; Tuan, H.-Y., Self-seeded growth of five-fold twinned copper nanowires: mechanistic study, characterization, and SERS applications. *Langmuir* **2014**, *30*, 602-610.
23. Ye, E.; Zhang, S. Y.; Liu, S.; Han, M. Y., Disproportionation for growing copper nanowires and their controlled self-assembly facilitated by ligand exchange. *Chem. Eur. J.* **2011,** *17*, 3074-3077.
24. Wang, C.; Hu, Y.; Lieber, C. M.; Sun, S., Ultrathin Au nanowires and their transport properties. *J. Am. Chem. Soc.* **2008,** *130*, 8902-8903.
25. Wang, C.; Hou, Y.; Kim, J.; Sun, S., A general strategy for synthesizing FePt nanowires and nanorods. *Angew. Chem. Int. Ed.* **2007,** *119*, 6449-6451.
26. Li, Q.; Zhu, W.; Fu, J.; Zhang, H.; Wu, G.; Sun, S., Controlled assembly of Cu nanoparticles on pyridinic-N rich graphene for electrochemical reduction of CO_2 to ethylene. *Nano Energy* **2016,** *24*, 1-9.
27. Schouten, K. J. P.; Qin, Z.; Pérez Gallent, E.; Koper, M. T., Two pathways for the formation of ethylene in CO reduction on single-crystal copper electrodes. *J. Am. Chem. Soc.* **2012,** *134*, 9864-9867.
28. Roberts, F. S.; Kuhl, K. P.; Nilsson, A., Electroreduction of carbon monoxide over a copper nanocube catalyst: surface structure and pH dependence on selectivity. *ChemCatChem* **2016,** *8*, 1119-1124.
29. Calle-Vallejo, F.; Koper, M. T., Theoretical considerations on the electroreduction of CO to C_2 species on Cu (100) electrodes. *Angew. Chem.* **2013,** *125*, 7423-7426.
30. Schouten, K. J. P.; Gallent, E. P.; Koper, M. T., The influence of pH on the reduction of CO and CO_2 to hydrocarbons on copper electrodes. *J Electroanal. Chem.* **2014,** *716*, 53-57.
31. Sandberg, R. B.; Montoya, J. H.; Chan, K.; Nørskov, J. K., CO-CO coupling on Cu facets: Coverage, strain and field effects. *Surf. Sci.* **2016,** *654*, 56-62.
32. Montoya, J. H.; Shi, C.; Chan, K.; Nørskov, J. K., Theoretical insights into a CO dimerization mechanism in CO_2 electroreduction. *J. Phys. Chem. Lett*. **2015,** *6*, 2032-2037.
33. Ma, S.; Sadakiyo, M.; Luo, R.; Heima, M.; Yamauchi, M.; Kenis, P. J., One-step electrosynthesis of ethylene and ethanol from CO_2 in an alkaline electrolyzer. *J. Power Sources* **2016,** *301*, 219-228.
34. Xiao, H.; Cheng, T.; Goddard III, W. A.; Sundararaman, R., Mechanistic explanation of the pH dependence and onset potentials for hydrocarbon products from electrochemical reduction of CO on Cu (111). *J. Am. Chem. Soc.* **2016,** *138*, 483-486.
35. Cheng, T.; Xiao, H.; Goddard III, W. A., Free-energy barriers and reaction mechanisms for the electrochemical reduction of CO on the Cu (100) surface, including multiple layers of explicit solvent at pH 0. *J. Phys. Chem. Lett*. **2015,** *6*, 4767-4773.

